Rearrangement of protein structures on a gold nanoparticle surface is regulated by ligand adsorption modes †

Xiaofeng Wang,[‡a] Rong Lei,[‡b] Limei Li,[‡a, c] Xinyu Fei,[c] Rui Ju,[c] Xiwen Sun,[c] Huiying Cao,[c] Qingfang Zhang,*[,a] Chunying Chen,*[, d] and Xinyi Wang*[,a, c]

[a] *School of Life Science and Biotechnology, Dalian University, Dalian, 116622, China.*

E-mail: wangxinyi163@163.com

[b] *Institute of Plant Quarantine, Chinese Academy of Inspection and Quarantine, Beijing, 100176, China.*

[c] *College of Land and Environment, Shenyang Agricultural University, Shenyang, 110866, China.*

E-mail: wangxinyi163@163.com

[d] *CAS Key Laboratory for Biomedical Effects of Nanomaterials and Nanosafety, &CAS Center for Excellence in Nanoscience, National Center for Nanoscienceand Technology of China, and University of Chinese Academy of Sciences, Beijing, 100190, China.*

† Electronic supplementary information (ESI) available. Material characterization, Protein adsorption analysis by DLS, Measurement of proteion secondary structures by ART-FTIR, Thermodynamic measurements by fluorescence quenching, and Computer simulation of the conformational changes and energy levels at nano-protein interface are all included in ESI.

‡ These authors contributed equally to this work.

Table S1. Methods and techniques for examining the structure and composition of protein corona.

Corona parameter	Techniques	References
Thickness	Transmission electron microscopy (TEM) [1-7], Dynamic light scattering (DLS)[1, 3, 5-14], Field Flow Fractionation (FFF)[15], Electrospray-Differential Mobility Analysis (ES-DMA)[16], Fluorescence correlation spectroscopy (FCS)[17], Small-angle X-ray scattering (SAXS)[18-20], Fluorescence correlation spectroscopy[21]	1-7, 14-21
Density	UV−Vis spectrophotometry[1, 7, 12], Scanning Electron Microscopy (SEM)[11, 22], Atomic force microscopy (AFM)[22]	1, 7, 11, 12, 22
Identity and quantity	SDS-PAGE[2, 5, 7-9], Liquid chromatography tandem mass spectrometry (LC-MS/MS)[5, 10, 13, 23, 24], ESI-MS[25]	2,5,7-9, 10, 13, 23-25
Conformation	CD spectroscopy[26, 27], Polarization modulation-infrared reflection–adsorption spectroscopy (PM-IRRAS)[6], Computational simulation[18, 28], Fourier transform infrared spectroscopy (FTIR)[27, 28], X-ray photoelectron spectroscopy (XPS)[11], Moleculardynamic (MD) simulation[14], Attenuated total reflection infrared spectroscopy(ART-IR)[14]	6,11,14,18,26-28
Affinity	Zeta potential[3, 11, 12, 23, 29], MP-SPR[6, 22], Isothermal titration calorimetry (ITC) [5], Electrophoretic light scattering (ELS)[10]	3,5,6,10-12, 22, 23, 29

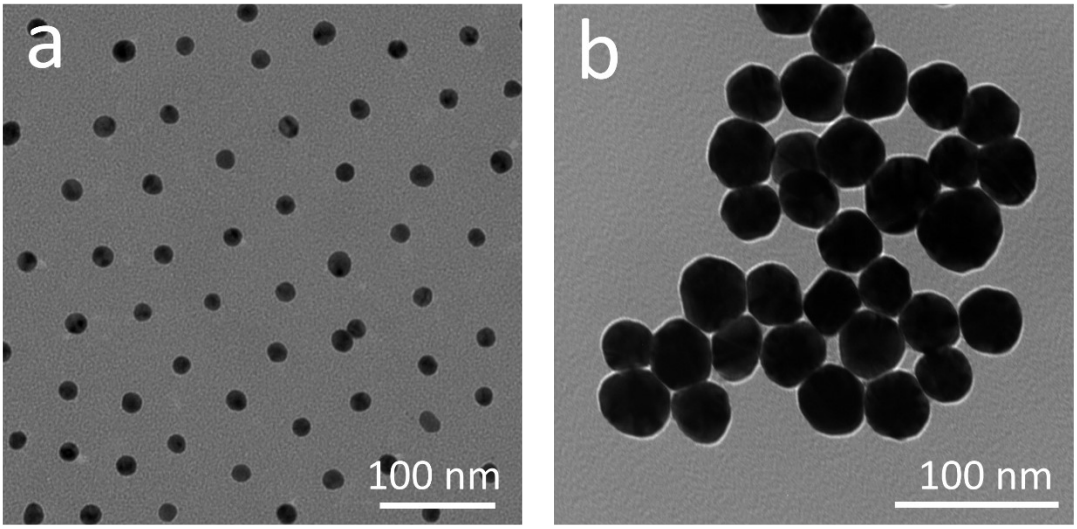

Fig. S1. Representative TEM image of Cit-AuNPs. (a) The average diameter of seed particles was measured to be 20 ± 2.6 nm (n=100). (b) The average diameter of Cit-AuNPs was measured to be 45.4 ± 3.9 nm (n=100).

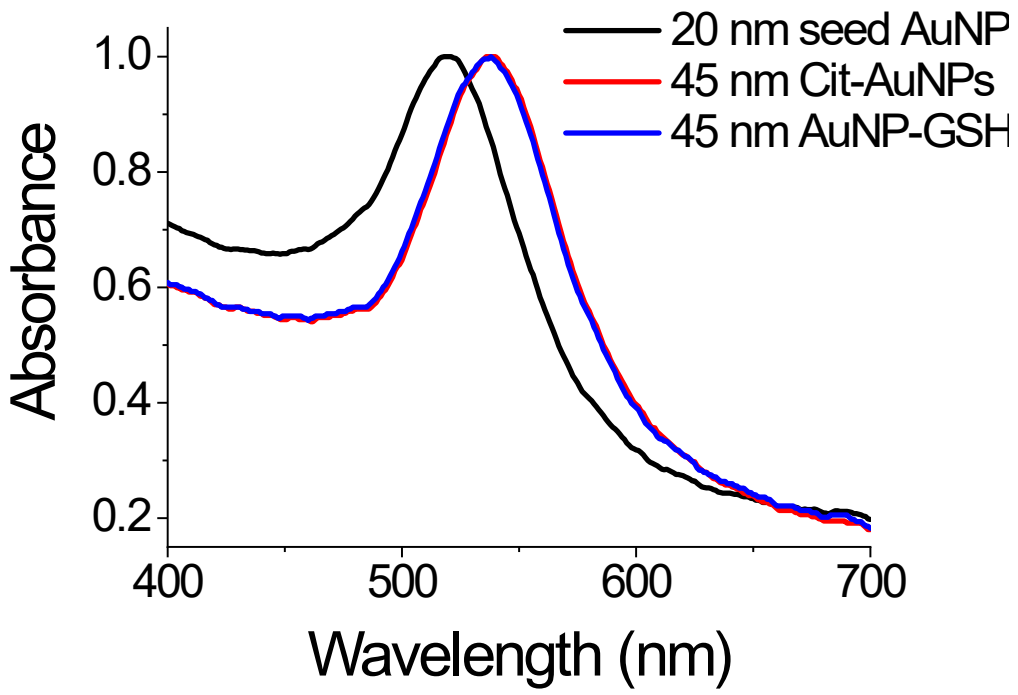

Fig. S2. The plasmon absorption spectra of AuNPs with various surface modifications.

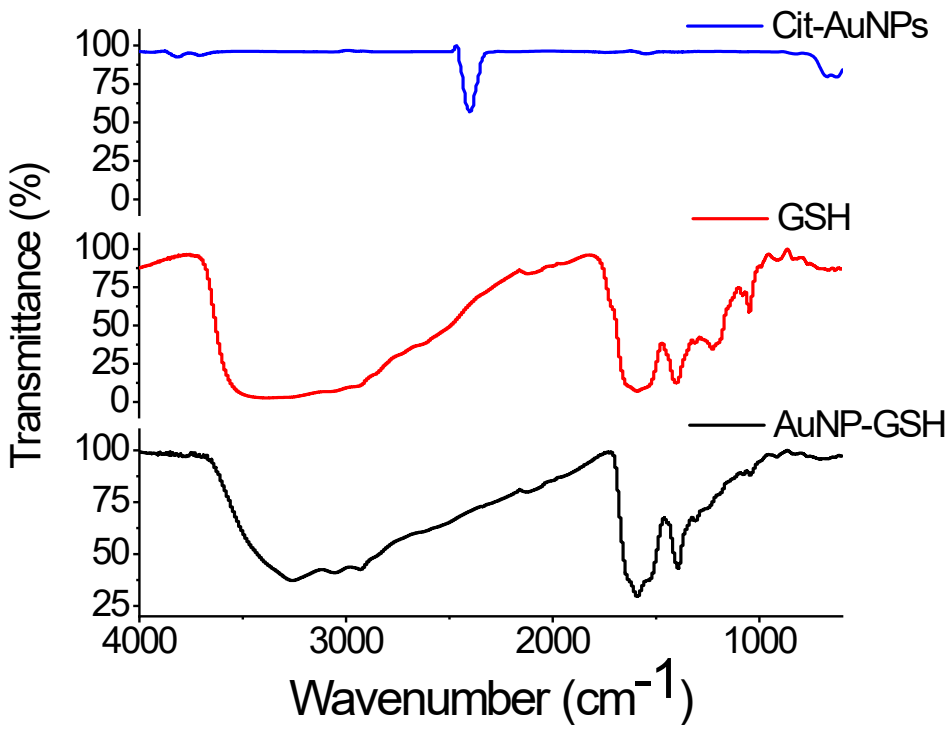

Fig. S3. FT-IR spectra of Cit-AuNPs and GSH-modified AuNPsv(AuNP-GSH). The characteristic peaks of GSH appeared in the spectrum of AuNP-GSH, indicate the chemical modification of GSH onto the surface of AuNPs.

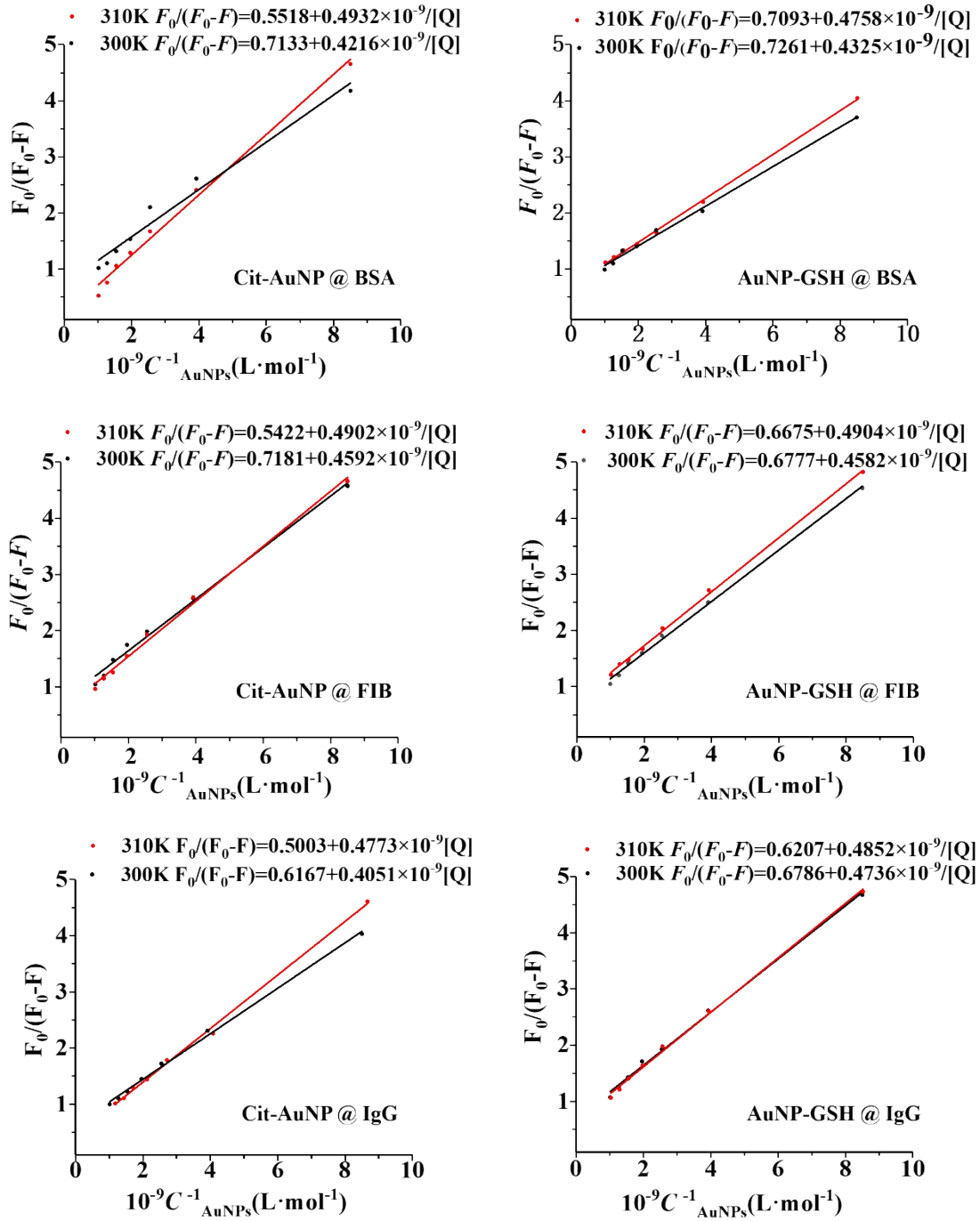

Fig. S4. Modified Stern-Volmer plots for the fluorescence quenching of three proteins by Cit-AuNPs or AuNP-GSH at different temperatures. The concentration of protein was fixed at 1.5μM and the concentrations of various AuNPs were from 0 to 15 nM.

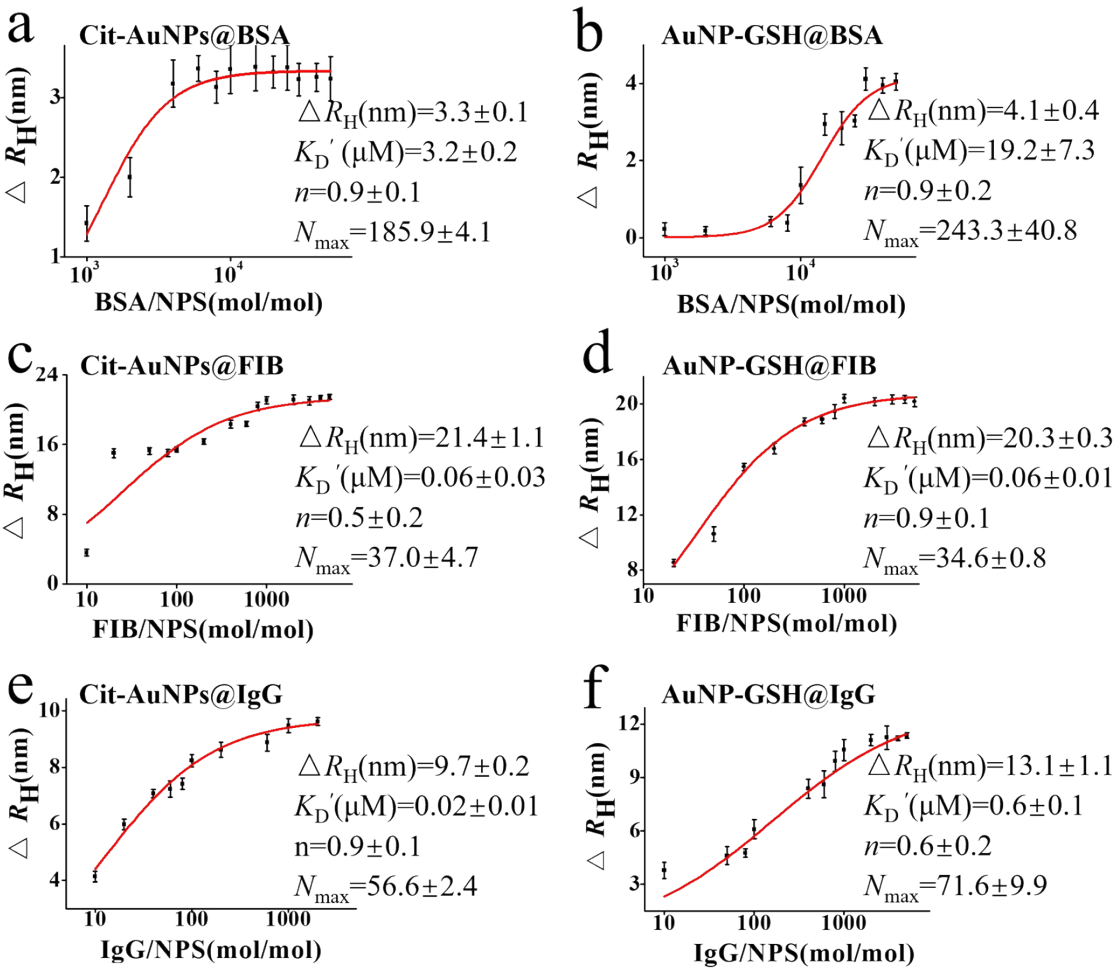

Fig. S5. Adsorption analysis of three plasma proteins onto Cit-AuNPs or AuNP-GSH. The hydrodynamic radius changes of Cit-AuNP@BSA (a), AuNP-GSH@BSA (b), Cit-AuNP@FIB (c), AuNP-GSH@ FIB (d), Cit-AuNP@IgG (e) and AuNP-GSH@ IgG (f), were plotted as a function of the corresponding concentrations of proteins, respectively. The final concentrations of all AuNPs (45 nm) were fixed at 1.5 nmol/L, and the DLS measurement was performed after incubating AuNPs with the desired concentrations of plasma proteins for 2 h at room temperature. The curves were fitted based on the Hill equation (red solid lines), and the best-fit parameters are listed on the right. All data are the mean±SD of three replicates.

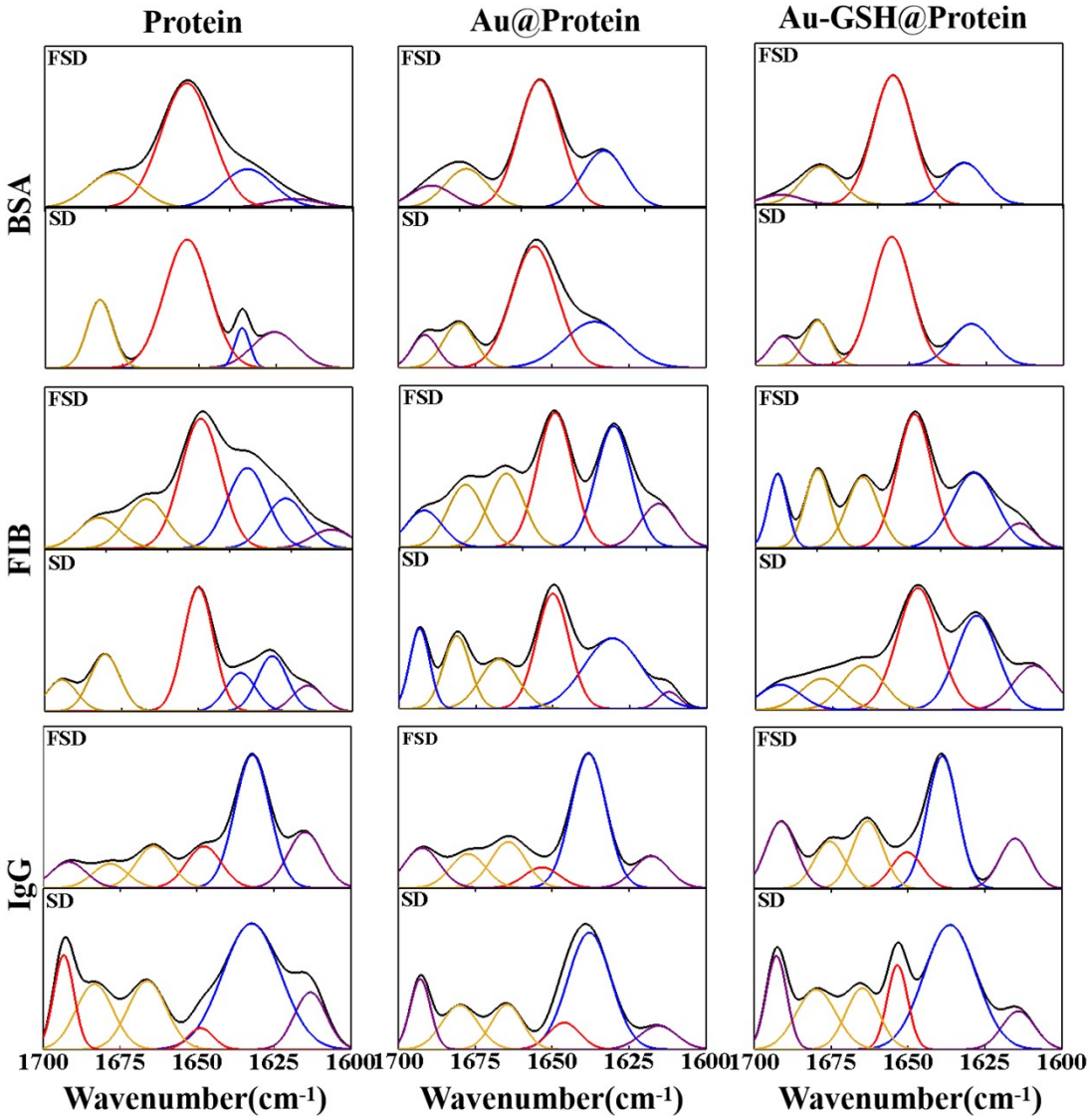

Fig. S6. ART-FTIR analysis of secondary structures of adsorbed plasma proteins on AuNPs with ligand-physisorbed or chemisorbed surfaces. Curve-fitted inverted SD and curve-fitted inverted FSD of amide I spectra were selected as the interest region for studying secondary structures of adsorbed proteins. The curve fitting was implemented by the OMNIC software (http://www.thermoscientific.com/en/ products/fourier-transform-infrared-spectroscopy-ftir.html).

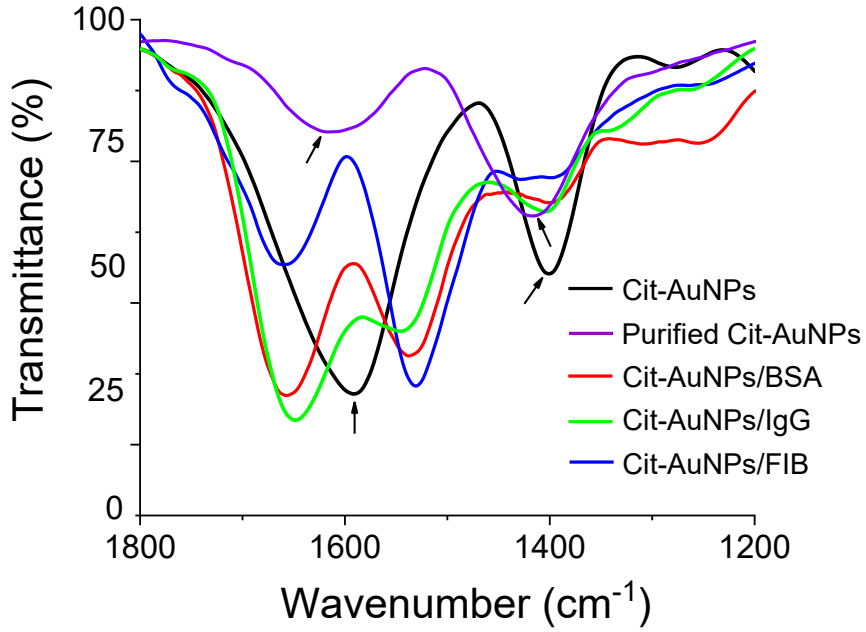

Fig. S7 ATR-IR spectra of Cit-AuNPs, purified Cit-AuNPs, and the Cit-AuNPs after incubating with excess proteins (BSA, IgG and FIB) at the frequency region of $\nu_{sy}(COO-)$ and $\nu_{asy}(COO-)$ vibrations. The peaks of $\nu_{sy}(COO-)$ at ~1590 cm^{-1} and $\nu_{asy}(COO-)$ at ~1390 cm^{-1} disappear upon the addition of the proteins (arrowed), indicating the replacement of citrates by the adsorbed proteins on the nanosurface.

Table S2. Percentage distributions of secondary structures of proteins before and after interaction with Cit-AuNPs or AuNP-GSH as determined by FTIR spectroscopy.

Protein	Method	Secondary structures (%)			
		α-helix	β-sheet	β-turn	other
BSA	X-ray[a]	74.9	3.1	1.4	20.6
	FSD[b]	61.0±2.0	13.8±1.5	17.3±0.5	7.8±0.5
	SD[c]	60.3±1.4	14.3±2.0	18.5±3.2	7.0±1.6
Cit-AuNPs@BSA	FSD[b]	52.6±3.2	21.5±1.6	18.2±2.3	7.7±3.6
	SD[c]	53.1±2.6	22.7±8.1	17.8±5.1	6.3±2.1
AuNP-GSH@BSA	FSD[b]	57.4±2.4	19.5±1.3	17.0±0.6	6.2±3.4
	SD[c]	58.2±2.3	18.9±1.8	15.0±2.3	7.9±1.1
FIB	X-ray[a]	\	\	\	\
	FSD[b]	35.5±2.5	35.4±2.1	13.5±0.3	15.6±3.5
	SD[c]	35.1±2.3	36.8±1.0	15.8±1.4	12.4±4.0
Cit-AuNPs@FIB	FSD[b]	27.1±2.3	39.1±1.8	18.2±3.5	15.6±2.9
	SD[c]	27.1±0.9	42.1±0.6	23.7±1.8	7.1±1.4
AuNP-GSH@FIB	FSD[b]	31.6±1.9	36.8±1.6	13.3±1.7	18.3±0.6
	SD[c]	31.8±1.7	37.7±1.3	15.0±1.2	17.5±1.5
IgG	X-ray[a]	\	\	\	\
	FSD[b]	14.3±1.3	42.4±1.4	29.9±2.3	13.4±1.3
	SD[c]	14.5±0.4	43.7±2.1	28.5±3.7	13.3±2.5
Cit-AuNPs@IgG	FSD[b]	8.8±2.2	47.2±3.1	28.1±3.1	15.9±4.0
	SD[c]	7.8±1.6	47.5±2.2	27.2±2.2	17.6±0.7
AuNP-GSH@IgG	FSD[b]	12.6±3.1	44.6±0.8	28.0±2.3	14.8±1.1
	SD[c]	12.2±1.1	45.8±3.1	31.4±3.1	10.6±1.1

[a]Data from X-ray structure; [b]Data from second-derivative FTIR analysis; [c]Data from Fourier self-deconvolution FTIR analysis.

Table S3. Assignment of amide I band frequencies to secondary structure of protein.

Mean frequencies(cm^{-1})	Secondary structures
1,624 ± 1.0	β-sheet
1,627 ± 2.0	β-sheet
1,633 ± 2.0	β-sheet
1,638 ± 2.0	β-sheet
1,642 ± 1.0	β-sheet
1,648 ± 2.0	Random
1,656 ± 2.0	α-helix
1,663 ± 3.0	3_{10}-helix
1,667 ± 1.0	β-turn
1,675 ± 1.0	β-turn
1,680 ± 2.0	β-turn
1,685 ± 2.0	β-turn
1,691 ± 2.0	β-sheet
1,696 ± 2.0	β-sheet

Table S4. The interaction energy at nano-protein interface.

Protein	On Cit-AuNP		On AuNP-GSH	
	Param1 (kJ/mol)	Param2 (kJ/mol)	Param1 (kJ/mol)	Param2 (kJ/mol)
BSA	-4365.02±96.26	-8672.37±87.18007	-538.70±109.10	-991.45±174.88
FIB	-7921.27±119.16	-14025.62±494.35	-2510.01±275.34	-3431.85±221.11
IgG	-5196.66±105.08	-12642.40±224.3	-1292.17±127.91	-1643.63±407.77

Table S5. Changes in the internal energy of protein at nano-protein interface.

Protein	Free protein (kJ/mol)	On Cit-AuNP		On AuNP-GSH	
		Param1 (kJ/mol)	Param2 (kJ/mol)	Param1 (kJ/mol)	Param2 (kJ/mol)
BSA	-76343.9 ± 291.4	-88037.4 ± 364.6	-86475.6 ± 331.5	-77594.9 ± 382.8	-77220.1 ± 435.8
FIB	-133984.3 ± 340.9	-135616.6 ± 640.9	-133341.6 ± 835.9	-135462.3 ± 379.1	-135145.6 ± 470.1
IgG	-134535.7 ±415.3	-136766.8 ± 599.1	-132995.9 ± 395.2	-136284.6 ± 487.8	-135873.1 ± 367.8

Table S6. Changes in the H-bond amount of protein at nano-protein interface.

Protein	Free protein	On Cit-AuNP		On AuNP-GSH	
		Param1	Param2	Param1	Param2
BSA	326.0 ± 4.5	374.4 ± 8.4	336.8 ± 10.2	348.9 ± 12.1	340.2 ± 11.3
FIB	543.9 ± 13.4	584.0 ± 15.0	547.5 ± 18.8	555.0 ± 13.9	558.5 ± 14.8
IgG	589.8 ± 16.7	619.8 ± 20.6	571.2 ± 16.0	606.6 ± 15.2	611.4 ± 16.8

Table S7. Changes in the salt-bridge amount of protein at nano-protein interface.

Protein	Free protein	On Cit-AuNP		On AuNP-GSH	
		Param1	Param2	Param1	Param2
BSA	66.1 ± 6.1	80.9 ± 6.6	74.1 ± 5.2	75.6 ± 6.8	75.4 ± 6.7
FIB	92.0 ± 6.2	109.8 ± 7.2	89.8 ± 6.7	109.5 ± 7.0	110.8 ± 7.1
IgG	71.9 ± 16.8	77.6 ± 6.2	67.8 ± 5.2	74.8 ± 7.6	64.2 ± 6.2

Table S8. MD simulating the formation of β-sheet structure of three proteins at nano-protein interface.

No.	On Cit-AuNP		On AuNP-GSH	
	FIB	IgG	FIB	IgG
1	ChainB-ASN411-Main……ChainB-VAL436-Main	ChainA-GLN16-Side……ChainA-SER13-Side	ChainB-CYS65-Main……ChainB-LEU75-Main	ChainA-ASN173-Side……ChainB-PRO171-Main
2	ChainB-ASP69-Main……ChainB-HIS67-Side	ChainA-ILE140-Main……ChainA-ALA178-Main	ChainB-ILE203-Main……ChainC-LEU218-Main	ChainA-GLU136-Main……ChainA-LEU182-Main
3	ChainB-GLY274-Main……ChainC-GLN136-Main	ChainA-LEU4-Main……ChainA-PHE101-Main	ChainC-GLY188-Main……ChainC-ASP185-Main	ChainA-ILE140-Main……ChainA-ALA178-Main
4	ChainB-THR280-Main……ChainB-TYR285-Main	ChainA-THR118-Main……ChainA-SER141-Main	ChainC-VAL143-Main……ChainC-ASP141-Side	ChainA-LEU182-Main……ChainA-GLU136-Main
5	ChainB-VAL436-Main……ChainB-ASN411-Main	ChainA-THR165-Side……ChainA-SER179-Main	ChainB-ILE227-Main……ChainB-TYR236-Main	ChainA-LEU184-Main……ChainA-ALA134-Main
6	ChainC-GLY188-Main……ChainC-ASP185-Main	ChainB-ALA141-Main……ChainB-SER131-Main	ChainB-SER222-Side……ChainB-MET242-Main	ChainA-LEU4-Main……ChainA-PHE101-Main
7	ChainC-THR224-Side……ChainC-HIS217-Main	ChainB-ALA363-Main……ChainB-MET413-Main	ChainB-ASN254-Main……ChainB-GLU291-Main	ChainA-SER180-Side……ChainA-SER179-Main
8	ChainA-THR107-Main……ChainA-ASN103-Main	ChainB-ARG40-Main……ChainB-GLU48-Main	ChainB-MET450-Main……ChainB-ARG255-Main	ChainA-SER183-Main……ChainA-GLY162-Main
9	ChainB-LEU302-Main……ChainB-LYS298-Main	ChainB-HIS414-Side……ChainB-ASP361-Main	ChainB-SER446-Side……ChainB-TYR417-Main	ChainA-SER69-Main……ChainA-THR72-Main
10	ChainC-ASP285-Main……ChainC-THR259-Main	ChainB-ILE321-Main……ChainB-TYR304-Main		ChainA-THR118-Main……ChainA-SER141-Main
11	ChainC-VAL122-Main……ChainC-ASN118-Main	ChainB-ILE362-Main……ChainB-SER360-Main		ChainB-ALA172-Main……ChainB-GLN109-Side
12		ChainB-LEU84-Main……ChainB-LEU18-Main		ChainB-ASN62-Side……ChainB-TRP49-Main
13		ChainB-LYS210-Side……ChainB-ASN208-Main		ChainB-ASP386-Main……ChainB-ASP384-Side

14	ChainB-SER184-Side……ChainB-THR169-Side	ChainB-ASP386-Side……ChainB-SER388-Side
15	ChainB-SER207-Side……ChainB-HIS204-Side	ChainB-LYS210-Side……ChainD-ASP212-Main
16	ChainB-THR379-Main……ChainB-TYR392-Main	ChainD-THR21-Main……ChainD-SER7-Main
17	ChainD-ASN62-Main……ChainD-ILE50-Main	ChainB-THR284-Side……ChainB-SER283-Main
18	ChainB-VAL185-Main……ChainB-HIS168-Main	ChainB-TYR281-Main……ChainB-THR284-Main
19	ChainB-VAL269-Main……ChainB-TRP262-Main	ChainB-TYR281-Main……ChainB-THR284-Main
20	ChainC-LEU139-Main……ChainC-THR120-Main	ChainC-LEU139-Main……ChainC-THR120-Main
21	ChainC-LEU184-Main……ChainC-ALA134-Main	ChainC-THR105-Side……ChainC-PRO7-Main
22	ChainC-THR166-Main……ChainC-SER179-Main	ChainD-GLN371-Side……ChainD-GLU373-Side
23	ChainC-TYR195-Main……ChainC-ALA211-Main	ChainD-ILE53-Main……ChainD-TRP36-Main
24	ChainD-GLN152-Side……ChainD-LEU112-Main	ChainD-LEU112-Main……ChainD-GLN152-Main
25	ChainD-THR135-Side……ChainD-THR139-Main	
26	ChainD-THR139-Side……ChainB-PRO276-Main	

Table S9. The number of disulfide bond, H-bond, salt-bridge and hydrophobic interaction of each protein.

Parameters	BSA	FIB	IgG
Disulfide bond	17	11	12
H-bond	326	544	590
Salt-bridge	63	92	72
Hydrophobic	52	88	105
aa	583	956	1288

References

1 C. Rodriguez-Quijada, H. de Puig, M. Sanchez-Purra, C. Yelleswarapu, J. J. Evans, J. P. Celli and K. Hamad-Schifferli, *ACS Appl. Mater. Inter.*, 2019, **11**, 14588-14596.

2 M. Hadjidemetriou, Z. Al-Ahmady, M. Mazza, R. F. Collins, K. Dawson and K. Kostarelos, *Acs Nano*, 2015, **9**, 8142-8156.

3 A. Cox, P. Andreozzi, R. Dal Magro, F. Fiordaliso, A. Corbelli, L. Talamini, C. Chinello, F. Raimondo, F. Magni, M. Tringali, S. Krol, P. J. Silva, F. Stellacci, M. Masserini and F. Re, *Acs Nano*, 2018, **12**, 7292-7300.

4 Z. Ban, P. Yuan, F. Yu, T. Peng, Q. Zhou and X. Hu, *Proc. Natl. Acad. Sci. U.S.A.*, 2020, **117**, 10492-10499.

5 J. Simon, L. K. Mueller, M. Kokkinopoulou, I. Lieberwirth, S. Morsbach, K. Landfester and V. Mailaender, *Nanoscale*, 2018, **10**, 10731-10739.

6 O. K. Kari, J. Ndika, P. Parkkila, A. Louna, T. Lajunen, A. Puustinen, T. Viitala, H. Alenius and A. Urtti, *Nanoscale*, 2020, **12**, 1728-1741.

7 G. Maiorano, S. Sabella, B. Sorce, V. Brunetti, M. A. Malvindi, R. Cingolani and P. P. Pompa, *Acs Nano*, 2010, **4**, 7481-7491.

8 K. Yang, B. Mesquita, P. Horvatovich and A. Salvati, *Acta Biomater.*, 2020, **106**, 314-327.

9 V. Francia, K. Yang, S. Deville, C. Reker-Smit, I. Nelissen and A. Salvati, *Acs Nano*, 2019, **13**, 11107-11121.

10 S. Palchetti, V. Colapicchioni, L. Digiacomo, G. Caracciolo, D. Pozzi, A. L. Capriotti, G. La Barbera and A. Lagana, *BBA-Biomembranes*, 2016, **1858**, 189-196.

11 S. Staufenbiel, M. Merino, W. Li, M.-D. Huang, S. Baudis, A. Lendlein, R. H. Mueller and C. Wischke, *Int. J. Pharmaceut.*, 2015, **485**, 87-96.

12 F. Xu, M. Reiser, X. Yu, S. Gummuluru, L. Wetzler and B. M. Reinhard, *Acs Nano*, 2016, **10**, 1189-1200.
13 V. Gorshkov, J. A. Bubis, E. M. Solovyeva, M. V. Gorshkov and F. Kjeldsen, *Environ. Sci-Nano*, 2019, **6**, 1089-1098.
14 X. Wang, X. Wang, M. Wang, D. Zhang, Q. Yang, T. Liu, R. Lei, S. Zhu, Y. Zhao and C. Chen, *Small*, 2018, **14**.
15 J. Ashby, S. Schachermeyer, S. Pan and W. Zhong, *Anal. Chem.*, 2013, **85**, 7494-7501.
16 J.-T. Tai, C.-S. Lai, H.-C. Ho, Y.-S. Yeh, H.-F. Wang, R.-M. Ho and D.-H. Tsai, *Langmuir*, 2014, **30**, 12755-12764.
17 C. Roecker, M. Poetzl, F. Zhang, W. J. Parak and G. U. Nienhaus, *Nat. Nanotechnol.*, 2009, **4**, 577-580.
18 T. Matsuo, *Biochem. Bioph. Res. Co.*, 2020, **525**, 830-835.
19 H. D. T. Mertens and D. I. Svergun, *J. Struct. Biol.*, 2010, **172**, 128-141.
20 P. Bernado and D. I. Svergun, *Mol. Biosyst.*, 2012, **8**, 151-167.
21 Z. Zeng, X. Shi, T. Mabe, S. Christie, G. Gilmore, A. W. Smith and J. Wei, *Anal. Chem.*, 2017, **89**, 5221-5229.
22 D. Maiolo, L. Paolini, G. Di Noto, A. Zendrini, D. Berti, P. Bergese and D. Ricotta, *Anal. Chem.*, 2015, **87**, 4168-4176.
23 K. Saha, M. Rahimi, M. Yazdani, S. T. Kim, D. F. Moyano, S. Hou, R. Das, R. Mout, F. Rezaee, M. Mahmoudi and V. M. Rotello, *Acs Nano*, 2016, **10**, 4421-4430.
24 A. J. Chetwynd, W. Zhang, J. A. Thorn, I. Lynch and R. Ramautar, *Small*, 2020, **16**.
25 H. Zhang, T. Wu, W. Yu, S. Ruan, Q. He and H. Gao, *ACS Appl. Mater. Inter.*, 2018, **10**, 9094-9103.
26 S. Kihara, N. J. van der Heijden, C. K. Seal, J. P. Mata, A. E. Whitten, I. Koper and D. J. McGillivray, *Bioconjugate Chem.*, 2019, **30**, 1067-1076.
27 X. Wang, M. Wang, R. Lei, S. F. Zhu, Y. Zhao and C. Chen, *ACS nano*, 2017, **11**, 4606-4616.
28 F. Tavanti, A. Pedone and M. C. Menziani, *Int. J. Mol. Sci.*, 2019, **20**.
29 J. Saavedra, S. Stoll and V. I. Slaveykova, *Environ. Pollut.*, 2019, **252**, 715-722.